EBioMedicine 48 (2019) 478–490

Contents lists available at ScienceDirect

EBioMedicine

journal homepage: www.elsevier.com/locate/ebiom

EBioMedicine
Published by THE LANCET

High urea induces depression and LTP impairment through mTOR signalling suppression caused by carbamylation

Hongkai Wang[a,b,#], Boyue Huang[a,#], Weiling Wang[a,#], Jinfang Li[c], Yi Chen[b], Trevor Flynn[d], Meng Zhao[c], Zhiming Zhou[e], Xiaojing Lin[f], Yinan Zhang[a,g], Mengmeng Xu[a], Keqiong Li[h], Kuan Tian[b], Dezhi Yuan[c], Peng Zhou[b], Ling Hu[b], Dandan Zhong[a], Shuai Zhu[a], Jing Li[b], Dilong Chen[b,i], Kejian Wang[b], Jianhui Liang[a,g], Qihua He[j], Jianbin Sun[k], Jie Shi[a,g], Li Yan[l], Jeff M Sands[m], Zhengwei Xie[a], Xuemei Lian[f], Duan Xu[d], Jianhua Ran[b,*], Baoxue Yang[a,*]

[a] *Department of Pharmacology, School of Basic Medical Sciences, and State Key Laboratory of Natural and Biomimetic Drugs, Peking University, Beijing, China*
[b] *Department of Anatomy, and Laboratory of Neuroscience and Tissue Engineering, Basic Medical College, Chongqing Medical University, Chongqing, China*
[c] *Department of Neurology, the Second Affiliated Hospital of Chongqing Medical University, Chongqing, China*
[d] *Department of Radiology and Biomedical Imaging, University of California, San Francisco, California, USA,*
[e] *Department of Radiology, the Second Affiliated Hospital of Chongqing Medical University, Chongqing, China*
[f] *School of Public Health and Management, Research Center for Medicine and Social Development, Innovation Center for Social Risk Governance in Health, Chongqing Medical University, Chongqing, China*
[g] *National Institute on Drug Dependence, Peking University, Bejing, China*
[h] *Chongqing Cancer Research Institute, Chongqing, China*
[i] *Chongqing Three Gorges Medical College, Chongqing, China*
[j] *Center of Medical and Health Analysis, Peking University, Beijing, China*
[k] *Clinical Laboratory, Peking University Third Hospital, Beijing, China*
[l] *Ion Channel Explorer Bioscience INC., Beijing, China*
[m] *Renal Division, Department of Medicine and Department of Physiology, Emory University School of Medicine, Atlanta, Georgia, USA*

ARTICLE INFO

Article history:
Received 4 July 2019
Revised 17 September 2019
Accepted 17 September 2019
Available online 15 October 2019

Keywords:
Urea
Depression
LTP
Carbamylation
mTOR

ABSTRACT

Background: Urea, the end product of protein metabolism, has been considered to have negligible toxicity for a long time. Our previous study showed a depression phenotype in urea transporter (UT) B knockout mice, which suggests that abnormal urea metabolism may cause depression. The purpose of this study was to determine if urea accumulation in brain is a key factor causing depression using clinical data and animal models.

Methods: A meta-analysis was used to identify the relationship between depression and chronic diseases. Functional Magnetic Resonance Imaging (fMRI) brain scans and common biochemical indexes were compared between the patients and healthy controls. We used behavioural tests, electrophysiology, and molecular profiling techniques to investigate the functional role and molecular basis in mouse models.

Findings: After performing a meta-analysis, we targeted the relevance between chronic kidney disease (CKD) and depression. In a CKD mouse model and a patient cohort, depression was induced by impairing the medial prefrontal cortex. The enlarged cohort suggested that urea was responsible for depression. In mice, urea was sufficient to induce depression, interrupt long-term potentiation (LTP) and cause loss of synapses in several models. The mTORC1-S6K pathway inhibition was necessary for the effect of urea. Lastly, we identified that the hydrolysate of urea, cyanate, was also involved in this pathophysiology.

Interpretation: These data indicate that urea accumulation in brain is an independent factor causing depression, bypassing the psychosocial stress. Urea or cyanate carbamylates mTOR to inhibit the mTORC1-S6K dependent dendritic protein synthesis, inducing impairment of synaptic plasticity in mPFC and

* Corresponding authors.
E-mail addresses: ranjianhua@cqmu.edu.cn (J. Ran), baoxue@bjmu.edu.cn (B. Yang).
[#] These authors contributed equally to this work.

https://doi.org/10.1016/j.ebiom.2019.09.049

depression-like behaviour. CKD patients may be able to attenuate depression only by strict management of blood urea.

Research in context

Evidence before this study

Urea transporter knockout mice showed depression-like behaviour with abnormal urea metabolism. However, it is not known whether or how extra urea contributes to depression.

Added value of this study

We identified the relevance between chronic kidney disease and depression. We find urea was sufficient to induce depression, to interrupt long-term potentiation (LTP) and to cause loss of synapses by impairing the medial prefrontal cortex.

Implications of all the available evidence

These data uncover the biological molecule urea as an important factor in depression. Furthermore, the unique mechanism may enable the discovery of new strategies for preventing and treating depression.

1. Introduction

Urea, the end product of protein metabolism, plays a vital role in the urine-concentrating process and water conservation in the mammalian kidney. It has been considered to have negligible toxicity for a long time. Elevated blood urea in chronic renal failure is thought to have no influence on survival in patients [1]. However, the view that urea is simply an innocent bystander was recently challenged by several new observations. High urea might have an important role in accelerated atherosclerosis in chronic dialysis patients [2]. It has also been reported that high urea increases levels of ROS and oxidative stress in cell lines [3] and mice [4]. Our previous work had discovered that urea transporter B (UT-B) null mice, in which urea accumulated in blood and brain, exhibited depression-like behaviour [5]. However, UT-As null mice, in which urea concentration was normal in blood, had no depression-like behaviour [6]. Thus, we hypothesized that urea accumulation in brain might cause depression.

Depression, characterised by a very low mood in all aspects of life and the inability to experience a sense of joy, is one of the most common and agonizing disorders globally [7]. Stress is generally considered the initial cause of the onset of, and a major contributor to, depression [8,9]. Patients who suffer from chronic physical diseases have a predisposition to depression versus the general public, which has been attributed to an increased stress level induced by physical and financial burdens [10,11]. However, another hypothesis suggests that chronic diseases might be etiologically related to depression through a pathophysiological mechanism [12,13]. Not surprisingly, when depression-related neural circuits in the brain are damaged by diseases such as stroke or Parkinson's, depressive symptoms often develop [14,15]. But to our knowledge, there is no convincing evidence that any physiological compound functionally causes depression, including both post-stroke or postpartum depression. We wondered whether high urea could cause depression through a primary biological mechanism. In this study, we tested the hypothesis that high urea in brain could induce depression in physiological and pathological conditions, independent of stress. The data in human subjects suggested a certain relationship between CKD and depression as expected and urea was the key factor responsible for depression by impairing the medial prefrontal cortex. In mice, urea was sufficient to induce depression-like behaviours and interrupt long-term potentiation (LTP) and cause loss of synapses in several models. The mechanism study showed that the hydrolysate of urea, cyanate, was involved in the mTORC1-S6K pathway inhibition, which was necessary for the effect of urea. Urea/cyanate concentrations could be sensed by mTOR. These data uncover a biological molecule urea as an important factor in depression. Furthermore, this unique mechanism may enable the discovery of new strategies for preventing and treating depression.

2. Materials and methods

2.1. Animals

7∼8-week-old C57BL/6J male and female mice were acclimated to Peking University, Beijing, vivarium for at least 7 days before experiments. Food and water were available *ad libitum*. They were housed in a colony room set at a constant temperature (23 °C) on a 12-h light/dark cycle (lights on from 08:00 to 20:00 p.m.). The behavioural tests were performed by experimenters who were blinded to the experimental group between 1:00 and 5:00 a.m. under red light. All protocols involving mice were approved by the Institutional Animal Care and Use Committee at the Peking University Health Science Center (Beijing, China).

Adenine-induced chronic kidney disease model was constructed as described with some modifications [16]. Briefly, mice were subjected to a 6-day induction phase by feeding them with 0.30% adenine and a 50-day maintenance phase by feeding a 0.15% and 0.20% diet in turn. Adenine was mixed with a casein-based diet that blunted the smell and taste (TP 1S000-003, Trophic Animal Feed High-Tech Co., Ltd, China). Other ingredients of the diet are maize starch (39.3%), casein (20.0%), maltodextrin (14.0%), sucrose (9.2%), maize/corn oil (5%), cellulose (5%), vitamin mix (1.0%), DL-methionine (0.3%) and choline bitartrate (0.2%). Total phosphate content was 0.9% and total calcium content was 0.6%. The control group was fed by the same casein-based diet without adenine. Mice were tested for behaviours in the subsequent 7 days after the maintenance phase.

Chronic carbamylation mouse model was established by drinking water containing 1 g/L sodium cyanate (Sigma) as described [17]. Antidepressants were administrated from the 5th week.

$A^{+/+};B^{-/-}$ mice were generated by crossing C57BL/6J background germline-heterozygous-null mutant $A^{+/+};B^{+/-}$ mice as described [18]. The offspring were genotyped by PCR using mouse-tail DNA and wild-type and mutant allele-specific primers (5′-AGGTGTGGCCTCAAAGTACTTGGCTA-3′). The PCR products were visualized with ethidium bromide staining.

$A^{-/-};B^{-/-}$ mice were generated by crossing C57BL/6J background germline-heterozygous-null mutant $A^{+/-};B^{+/-}$ mice as described [19]. The offspring were genotyped by PCR using mouse-tail DNA and wild-type and mutant allele-specific primers (5′-GAGAGGTGAGACCGCAGAAT-3′; 5′-CACCTGTATGTGGTCCAGCAA-3′; 5′-GATGTGGAATGTGTGCGAGG-3′). The PCR products were visualized with ethidium bromide staining.

Mice were killed after behavioural tests, and the blood was collected and centrifuged for reserve. mPFC urea was measured by

using QuantiChrom Urea Assay kit (Roche Diagnostics, Indianapolis, IN, USA). Serum was measured in a clinical laboratory of Peking University Third Hospital.

2.2. Serology

The mice were euthanized and then the plasma (extirpate/remove the eyeball, and then the plasma was collected by the ophthalmic vein) was collected for tests. The collected plasma was incubated for 30 min (room temperature), then centrifuge for 10 min (3000 rpm). The following measuring methods for the detection of a substance in serum samples were used. Uric acid concentrations were determined by using a uricase method (SHINOTESTCORPORATION, Japan). Urea by urease-glutamate dehydrogenase method (Baiding Biological Engineering (Beijing) Co.,Ltd.). Calcium by ocresolphthalein complex ketone method (BIOSINO BIOTEC). Creatinine by picric acid method (YANTAI AUSBIO LABORATORIES CO,.LTD.). Phosphate by phosphomolybdate method (BIOSINO BIO-TEC). The measurements were performed using the biochemical analyzer (AU5800 comes with ion test reagent, Beckman Coulter Commercial Enterprise Co., Ltd.) to detect potassium, sodium and chloride.

For human samples, all biochemical tests were performed at the Department of Clinical Laboratory in the Second Affiliated Hospital of Chongqing Medical University. Before the MR imaging, blood samples were collected by venipuncture into the heparin treated centrifuge tubes and placed statically for 30 min. Plasma was recollected by centrifugation at 3000 rpm for 15 min. Serum chemistry values, which included serum creatinine level, urea level, serum uric acid level, serum sodium level, serum potassium level, serum calcium level, serum chloride level, serum phosphate level, hemoglobin level, cholesterol level, serum albumin level, serum triglyceride level, serum low density lipoprotein level, serum glucose level, serum lipoprotein level, and serum parathyroid hormone level were measured using an autoanalyzer with standard procedures (Hitachi 7600 Automatic Biochemical Analyzer; Hitachi Co. Ltd, Tokyo, Japan).

2.3. Drugs and virus

Ketamine (the First People's Hospital of Chongqing Liang Jiang New Area) was administered i.p. at a concentration of 3 mg kg^{-1}. Constitutively active (S6K-T389E-ΔCT) mutants of S6K were developed in Likeli Technologies followed by a previous study [20]. Mice were tested one month after AAV injections.

2.4. Stereotaxic injection

Constitutively active S6K in the mPFC was achieved by injecting AAV2 vectors expressing single mutant mouse S6K, as well as green fluorescent protein (GFP). AAV2-GFP was used as a control. Sodium pentobarbital (60 mg/kg, i.p.) was used to anaesthetize the mice before they were bilaterally implanted with permanent guide cannulae (outer diameter, 0.41 mm; inner diameter, 0.25 mm; RWD Life Science, Shenzhen, China) in the mPFC (anterior/posterior, +1.75 mm; medial/lateral, ±0.75 mm; dorsal/ventral, −2.65 mm at 15° angle). The virus was intracranially microinjected using 10 μl Hamilton syringes (Hamilton, Reno, NV, USA) that were connected via polyethylene-50 tubing (outer diameter, 0.61 mm; inner diameter, 0.28 mm; RWD Life Science) to injectors (outer diameter, 0.21 mm; inner diameter, 0.11 mm; RWD Life Science). For viral infusions, a total volume of 0.5 μl was infused into each side over 5 min, and the injection syringe was left in place for an additional 5 min to allow for diffusion.

2.5. Behaviour tests

Detailed materials and methods of coat score assay, sucrose preference test, open field test (OFT), forced swimming test (FST), elevated plus maze (EPM), novelty suppressed feeding test (NSFT), tail suspension test (TST) and splash test were provided in the **Supplementary Information**. Multiple behaviour tests were used on the same animals. All animals from different groups were given the same tests in the same order.

2.6. Electrophysiology

Acute brain slices were prepared from the prefrontal cortex in mice. Mice were deeply anaesthetized with ether (4 ml) and decapitated. The brain was rapidly removed from the skull with the least amount of damage and pressure onto the brain. Then the brain was transferred into the ice-cooled artificial cerebrospinal fluid (ACSF) (in mM: 124 NaCl, 2.5 KCl, 1.2 NaH_2PO_4, 24 $NaHCO_3$, 12.5 D-Glucose, 2 $CaCl_2$, and 1.5 $MgSO_4$ saturated with 95% O_2 and 5% CO_2 to pH: 7.3.). A filter paper was placed on the bottom of one petri dish in advance. Using the spoon, the brain was transferred into the petri dish containing ice-cold ACSF and placed the ventral side of the brain touching the filter paper. Transversal slices with 400 μm thickness containing hippocampus were cut with a Vibratome (Leica, VT 1000 S, Germany), which was filled with the cold ACSF. The prepared slices were incubated in oxygenated ACSF at room temperature at least for 1 h, and then individual slices were transferred to a recording chamber, which was bubbled with oxygenated ACSF at 31 ± 1 °C.

The perfusion rate was adjusted to 2 ml/min. The electrophysiological recordings were obtained under visual control by use of an Olympus microscope (Olympus BX50-WI, Olympus, Japan) and a 40x long-working distance objective (NA 0.8).

The detail of the fEPSP and mEPSC is provided in **Supplementary information**.

Each set of data was tested to determine whether the distribution fits a normal distribution. If not otherwise noted, parametric Student's *t*-test was performed for statistical evaluation of the data. Unpaired *t*-test was used. Results are presented as mean ± s.e.m., and differences were considered significant if $p < 0.05$. Cumulative distribution plots of mEPSCs amplitudes and interevent intervals were compared with the Kolmogorov-Smirnov test. Probability values of < 0.05 were considered significant.

2.7. Neuron culture

Newly postnatal C57bl/6j mice were purchased from the Department of Laboratory Animal Science, Peking University Health Science Center, Beijing. Anaesthetized mice were sacrificed by cervical dislocation. All tissues were maintained in D-Hank's solution (KCl 0.4 g, KH_2PO_4 0.06 g, NaCl 8.0 g, $NaHCO_3$ 0.35 g, $Na_2HPO_4 \cdot 12H_2O$ 0.132 g, D-Glucose 1.0 g in 1 L $dddH_2O$, pH 7.4) and chilled on ice. The dissected medial prefrontal cortex was centrifuged (1000 r/min, 7 min, room temperature) after dispersed by trituration and 0.25% trypsin digestion (Hyclone. 5 min, 37 °C). Culture medium was DMEM (Gibco) supplemented to 10% FBS (Gibco) for the first 4 h, then changed to neurobasal (Gibco) with 2% B27 (Gibco) and 0.5 mM L-glutamine (Sigma). Cells were plated on 0.1% poly-L-lysine (Sigma, for urea stimulation) or poly-ornithine (Sigma, for cyanate, because cyanate is fast reacted with residue of lysine) coated 10 cm dishes or 6-well plates at 1×10^6 cells/ml of medium, and maintained in an incubator at 37 °C and 5% CO_2. Urea (Sigma), mannitol (Sigma), sodium cyanate (Sigma) and sodium chloride (Sigma) were dissolved into the medium for stimulation. Neurons after cultured for 15 days was subjected to subsequent experiments.

2.8. Western blot

Tissues or cells were homogenized in RIPA lysis buffer (Thermal Scientific) containing protease inhibitor cocktail (Roche). The extract was homogenized using a Dounce homogenizer and spun at 12,000 g for 20 min at 4 °C. Total protein was measured by BCA (Pierce) and resolved by sodium dodecyl sulfate–polyacrylamide gel electrophoresis (SDS-PAGE). Proteins were blotted to polyvinylidene difluoride membranes (Amersham Biosciences). Blots were incubated with polyclonal antibody against S6 (CST), p-S6 (CST), S6K (CST), p-S6K (CST), mTOR (CST), p-mTOR (CST), Synapsin-1 (CST), PSD95 (Abcam), MAP2 (Abcam) and β-actin (Santa Cruz). Goat anti-rabbit IgG (Scicrest), goat anti-mouse IgG (Scicrest) were added, and the blots were developed with ECL Plus Kit (Amersham Biosciences). Relative protein expression was quantified by optical density.

2.9. Carbamylation pull-down

Tissues were homogenised in RIPA lysis buffer (Thermal Scientific) containing protease inhibitor cocktail (Roche). The extract was homogenised and spun at 12,000 g for 20 min at 4 °C. Pre-cleared lysates were incubated with anti-carbamylation antibody (Abcam, ab175132) coupled to protein A/G agarose (Santa Cruz) overnight at 4 °C. The immune complex was collected by centrifugation, and the pellets were washed in lysis buffer three times for 10 min with rotation at 4 °C. Carbamylated proteins were washed with cold lysis buffer six times, resuspended in SDS sample buffer, and subjected to SDS-PAGE and Western blot analysis.

2.10. Immunofluorescence

The mice were deeply anaesthetized with pentobarbital (85 mg/kg, i.p.) and perfusion with 20 ml of 0.9% saline, followed by 20 ml of fresh 4% paraformaldehyde in 0.01 M phosphate buffered saline (pH 7.3). After perfusion, brains and kidneys were taken out for an additional fixation overnight in the same 4% paraformaldehyde, followed by a graded series of sucrose gradient dehydration. Dehydrated samples were frozen to be sectioned in the coronal plane at 20 μm for immunofluorescent detect or direct observation of GFP (Leica). Slices were subsequently washed by PBS for 5 min thrice. Then the slices were washed in PBS–T (0.3% Triton X–100 in PBS) for 0.5 h at 37 °C and transferred to blocking solution (0.3% PBS–T in 5% goat serum) overnight at 4 °C before ~36 h incubation (0.3% PBS–T in 1% serum) in primary antibody solution (rabbit anti–UT-B, a gift from Dr. Trinh-Trang-Tan MM [21]; and rabbit anti-UT-A1, previously home-made). Slices were then washed in PBS thrice and incubated for 0.5 h with secondary antibody (Cy3 goat anti-rabbit IgG 1:200, Invitrogen; Hoechst 1:1000, Leagene) for fluorescent detection. Fluorescent image acquisition was performed with a Leica TCS SP8 confocal laser microscope.

2.11. H&E staining

The kidneys of mice were removed carefully, rinsed with 0.01 M PBS three times, and put into 4% paraformaldehyde solution for 24~48 h at room temperature. The tissues were rinsed with running tap water for 1 h, followed by the dehydration of the tissue through 70%, 80%, and 95% alcohol for 45 min each, and 100% alcohol for 1 h. The tissues were cleared through 2 changes of xylene for 1 h each and immersed in 3 changes of paraffin for 1 h each, followed by embedding in a paraffin block. The paraffin-embedded tissue blocks were sectioned at 5 μm thickness on a microtome and buoyed in a 40 °C water bath containing distilled water to transfer onto glass slides for drying until ready for use. Sections were then deparaffinised in xylene and rehydrated through graded alcohols to water and stained with haematoxylin and eosin using standard procedures. The sections were examined by light microscopy (Olympus, Japan) for histological analysis.

2.12. Meta-analysis

We searched the Cochrane Library, MEDLINE, and Embase for articles published before March 1st, 2016. The keywords for searching are provided in the **Supplementary Information**. The inclusion criteria for selection of published studies for this meta-analysis were as follows: (1) exact number of ratios described the mortality of depression in people with clinical physical illness; (2) studies designed as an observational study; (3) the depression was diagnosed by CES-D, BDI or HADS scales. Several investigators independently extracted data from the selected studies, based on the predetermined selection criteria, and any disagreements were resolved by discussion and reexamination. The following information was extracted: first author, publication date, country, sample size, sex of subjects, specific primary diseases, study tools for assessment of depression, cut point for diagnosis of depression, and number of cases. R software was used to merge respectively. Because $I^2 > 50\%$ and $P < 0.1$, random-effects model was employed for the analysis. In order to compare these three results, SPSS software was used for chi-square test.

2.13. Human subjects

Medical research ethics committee approval and written informed consent were obtained. A total of 40 patients with CKD were enrolled in the Department of Nephrology, the Second Affiliated Hospital of Chongqing Medical University from Sept. 2016 to Jan. 2017, divided into two groups according to depression and non-depression. There were 19 males (47.5%) and 21 females (52.5%), aged 32~76 years, mean age 51.1 ± 11.8 years. Inclusion criteria:(1) patients at uremic stage of chronic renal failure (CRF); (2) the blood Cr >707 mM and endogenous creatinine clearance <15 ml / (min • 1.73 m^2); (3) patients with normal liver function and the plasma glucose range at 5.4 ~ 13.2 mmol/L level; (4) cranial MRI has no new lesions; (5) patients have no drug or food poisoning and psychiatric history. Exclusion criteria: (1) patients had been diagnosed with brain tumours, brain trauma, dementia, confusion; (2) patients had been diagnosed with severe infection, acute left ventricular failure, other severe complications and the presence of other organs severely damaged; (3) patients who cannot effectively complete the questionnaire. The enlarged CKD patient cohort included 176 participants. There were 86 males (48.9%) and 90 females (51.1%), aged 17~95 years, mean age 61.0 ± 17.2 years.

Healthy control subjects (HCs) with similar age and sex distribution to those CKD patients were recruited from the outpatient physical examination. There was no history of psychosis or similar family history. Among them, 5 were male (33.3%) and 10 were females (66.7%), aged from 33 to 72 years, mean age 56.4 ± 12.3 years old. There was no significant difference in gender and age between the three groups ($P > 0.05$).

Each patient completed questionnaires before the MRI examination, including age, sex, years of education, duration of hemodialysis and Hamilton Rating Scale for Depression (HAMD) and Hamilton Anxiety Scale. The healthy control subjects were also asked about their general situation and evaluated for depression.

MRI data acquisition method was shown in detail in **Supplementary information**.

2.14. Statistical analyses

All data are presented as mean ± s.e.m. Data were analysed using two-tailed Student's *t*-tests (for two-grouped comparisons)

or ANOVA (for multiple-group comparisons). Significance was assigned at $P < 0.05$. $^{*}P < 0.05$, $^{**}P < 0.01$, $^{***}P < 0.001$. n.s., not significant. In all the figures, *n* refers to the sample sizes when applicable. Sample sizes were selected based on previous experiments. Unless otherwise indicated, results are based on at least three independent experiments to guarantee reproducibility of findings. Unless otherwise mentioned, statistical analyses were performed using Graphpad Prism software.

3. Results

3.1. Urea accumulation impairs mPFC to induce depression in chronic kidney disease patients

We did 3 meta-analyses of ~40,000 human participants to compare co-morbidities of depression secondary to CKD, and employed another three common severe chronic organ failures as contrasts: chronic obstructive pulmonary disease (COPD), liver cirrhosis and chronic heart failure (CHF) (Supplementary Fig. 1). Unfortunately, the lack of original studies on liver cirrhosis made it unable to be included in the analysis. As organ transplantation tremendously changes the status of end-stage diseases, we excluded all data from those patients. We also excluded data of patients with brain diseases that may directly affect mood-related brain circuits. We separately analysed the co-morbidity of depression diagnosed by 3 different types of scales that were abundantly used. By the Hospital Anxiety and Depression Scale (HADS), a total of 28 studies (17 of CKD, 7 of COPD, 4 of CHF) including 4113 adult participants from 15 countries were included (Supplementary Figs. 1, 2, and Supplementary Table 1). A random-effect model was employed for the analysis, due to $I^2 > 50\%$ and *p*-value < 0.1. The co-morbidity after CKD was much higher than the other two chronic diseases that were selected for this study (Fig. 1a). By Beck Depression Inventory (BDI), a total of 36 studies (18 of CKD, 5 of COPD, 13 of CHF) including 17,753 adult participants from 15 countries were included, and by Center for Epidemiologic Studies Depression Scale (CES-D), a total of 23 studies (10 of CKD, 4 of COPD, 9 of CHF) including 18,446 adult participants from 8 countries were included (Supplementary Figs. 1, 3, 4 and Supplementary Tables 2, 3). The co-morbidity after CKD was much higher than after CHF or COPD, respectively (Supplementary Figs. 3d, 4d). We thus targeted the causal relation between CKD and depression, and we speculated that high urea, other than stress, may play an more important role in CKD-related depression.

Next, we determined the brain regions that were impaired by CKD. Multiple studies unveiled that the prefrontal cortex (PFC) is heavily implicated in depression-related brain regions [22,23]. However, whether PFC is impaired by CKD, similarly to stress, was unknown. Thus, we recruited 40 hemodialysis patients with healthy community samples (Supplementary Table 4). Physicians quantified their mood condition by Hamilton Depression Rating Scale (HAMD) and Hamilton Anxiety Scale. Patients with mania attack were excluded. CKD patients were separated into a depressed group ($n = 19$) and a non-depressed group ($n = 21$) with a cut-off value at score 17 in HAMD (Fig. 1b). Serum urea and creatinine levels were increased in CKD patients, and urea level was slightly higher in the depressed group than the non-depressed group (Fig. 1c, d). Moreover, the extent of depression in the CKD population highly correlated with the extent of anxiety (Fig. 1b). To confirm the responsible uremic toxin, we enlarged our hemodialysis patient cohort to 176 participants and examined the difference between depressed and non-depressed groups (Supplementary Table 5). Common biochemical indexes were measured, but only urea was significantly higher in the depressed group (Fig. 1e).

Impaired PFC by CKD was unveiled by the group differences in frontal cortex connectivity as measured by resting-state fMRI. The depressed CKD group exhibited aberrant frontal cortex functional connectivity relative to both the non-depressed CKD and healthy control groups at each of the three ROIs. These aberrances included increased connectivity between the medial PFC (mPFC) and left precuneus, decreased connectivity between the mPFC and sections of the dorsolateral PFC and posterior cingulate cortex (Fig. 1f); increased connectivity between dorsolateral PFC and cuneus, precentral cortex and insular cortices, and decreased connectivity between the right dlPFC and caudate nucleus and contralateral superior frontal gyrus (Supplementary Fig. 5). These clusters were generally slightly larger in the depressed CKD versus healthy control comparison than in the depressed CKD versus non-depressed CKD (Fig. 1f and Supplementary Fig. 5). The impairment of PFC appeared before the depressive symptoms appeared, suggesting the impairment of PFC by CKD is the cause but not the result of depression. Together, CKD impairs PFC to induce depression, which is similar to stress.

3.2. High urea in mPFC causes depression in CKD mice

To determine whether high urea has a role in facilitating depression, we verified the behaviours of mice that mimicked human CKD. Animal models excluded social-psychological stressors, such as financial burden, that complicates the human studies, so that only biological factors are left. To minimise potential confounding factors, we chose a mild chemical-induced CKD mouse model instead of a surgical one, as exposure to stress tends to induce depression-like phenotypes in mice [24]. The nephrotoxin adenine was mixed into routine diets to permit mouse behaviour uncontaminated by unnecessary stress. Adenine was fed continuously for 8 weeks following one-week habituation as described (Supplementary Fig. 6a). Mice fed with adenine showed much higher serum urea and higher creatinine values, which represent kidney dysfunction (Fig. 2a, b). Though mice were overloaded with adenine, uricase kept their uric acid level at the normal level (Supplementary Fig. 7a). We also analysed blood electrolytes and found serum sodium, potassium, phosphate, and chloride were at normal levels (Supplementary Fig. 7b, c, e, f). CKD mice have elevated serum calcium with intact adjusted kidney index (Supplementary Fig. 7d, g). Kidney histology exhibited deposition of symmetric crystalline structures in tubular lumen and microabscesses (Supplementary Fig. 8). Kidney damage was mainly tubulointerstitial due to peritubular leukocyte infiltration and interstitial/peritubular oedema (Supplementary Fig. 8). Further, according to the MRI results, it was revealed that the main altered brain region in urea-induced depression was the prefrontal cortex. So we tested and found that the urea level was higher in mPFC of CKD mice (Fig. 2c). The results confirmed successful construction of an mPFC urea accumulation model in mice.

In a sucrose preference test, sucrose consumption was decreased in the CKD mice relative to control, which showed anhedonia, a core symptom of depression (Fig. 2d). Mice that had CKD also exhibited increased immobility in the forced swimming (Fig. 2e) and tail suspension tests (Supplementary Fig. 7m), which showed despair, another symptom of depression. Latency of immobility increased in the tail suspension test (Supplementary Fig. 7n). In contrast, a motor defect did not appear in CKD mice by open field test (Supplementary Fig. 7h–k). Coat score, monitored weekly, resulted in deterioration (Fig. 2f). Two distinct well-characterised antidepressants, imipramine (tricyclic antidepressant) and ketamine (rapid-acting antidepressant), were administrated to CKD mice. The two antidepressant groups with imipramine and ketamine showed improved anhedonia and despair symptoms (Supplementary Fig. 7m). The antidepressants also

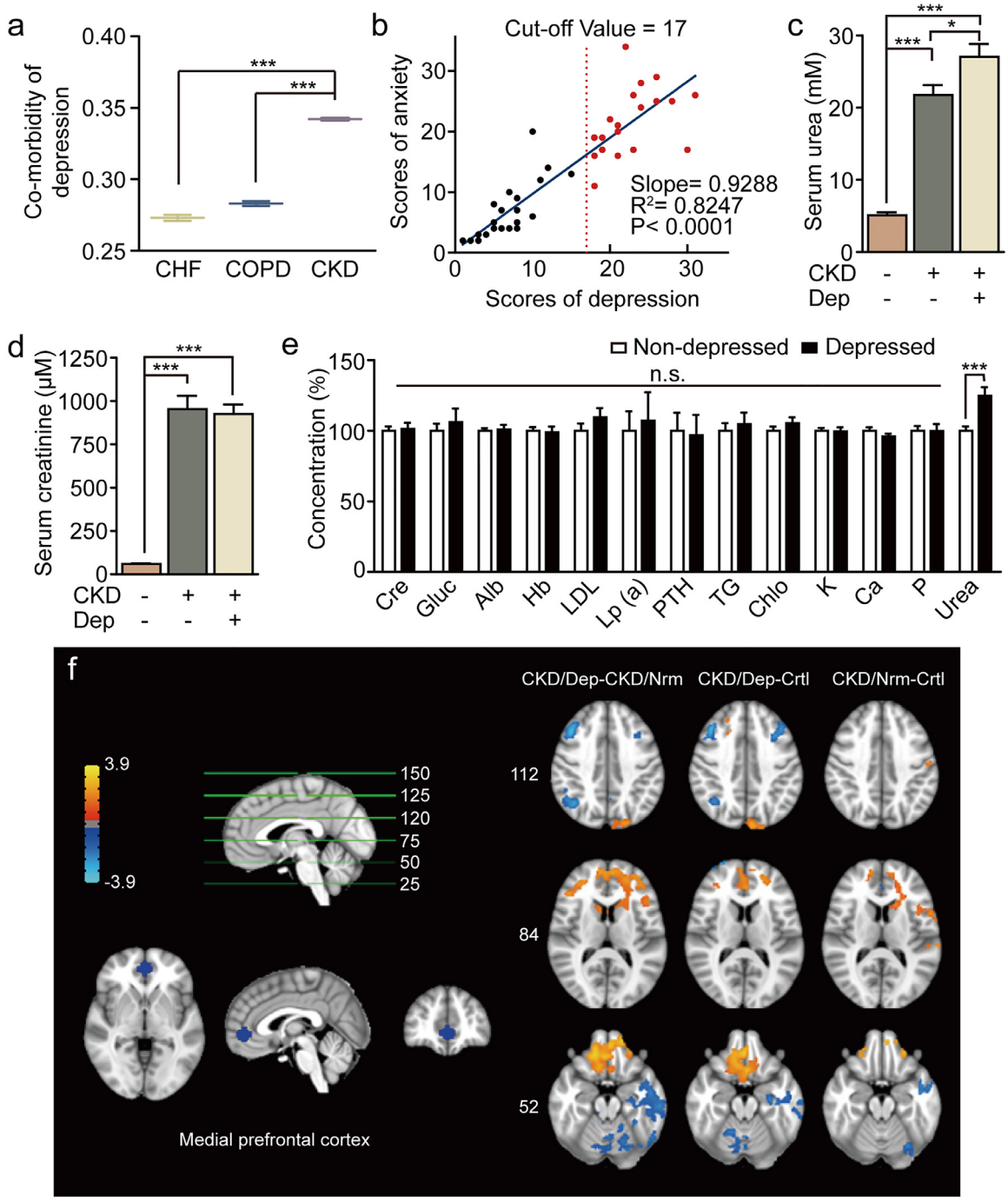

Fig. 1. Urea accumulation impairs mPFC to induce depression in chronic kidney disease patients. a, Diagram of co-morbidity of depression secondary to CKD, COPD and CHF. Chi square test. b, Correlation between depressive symptoms and anxious symptoms. Red dotted line, cut-off value of Hamilton Depression Rating Scale. Red spots, each representing a CKD patient diagnosed as depression ($n = 19$). Black spots, each representing a CKD patient excluded from depression ($n = 21$). c, Serum urea level of participants ($n = 15, 21, 19$). d, Serum creatinine level of participants ($n = 15, 21, 19$). e, Screening of index on enlarged CKD patient's cohort. CKD patients without depression group was adjusted to 100%. Cre, creatinine; Gluc, glucose; Alb, albumin; Hb, hemoglobin; LDL, low-density lipoprotein; LP(a), lipoprotein(a); PTH, parathyroid hormone; TG, triglyceride; Chlo, chloride ions; K, potassium ions; Ca, calcium ions; P, phosphate ions. Specific numbers are in the Supplementary Table 5. f, Differences in mPFC resting-state functional connectivity between depressed CKD (CKD/Dep), non-depressed CKD (CKD/Nrm) and healthy control (Ctrl) groups ($n = 20, 21, 19$). mPFC ROI locations are in blue. Axial slice level indicated in the z-axis with 1 mm MNI space. Orange clusters represent regions of significantly higher connectivity in the first group, blue clusters significantly lower (the bar). Clusters obtained from t-tests of the seed-voxel correlation z-score maps for each pair of groups. Resulting t-score maps thresholded and clusterized at voxelwise $p = 0.05$, cluster $\alpha = 0.05$.

markedly improved the physical state of the coat score with acute or chronic onset (Fig. 2f) in agreement with previous studies [24–27]. Imipramine and ketamine did not affect any kidney-related index, so their positive effects were not resulting from amelioration of kidney damage (Supplementary Fig. 7, 8). These results support the existence of depression-like phenotypes in CKD mice.

3.3. High urea sufficiently induces depression and impairs long-term potentiation (LTP) in mPFC

Next, we studied a mouse model with simple high-level urea but normal kidney function. High urea would not lead to any abnormalities that caused discomfort, so this model excluded

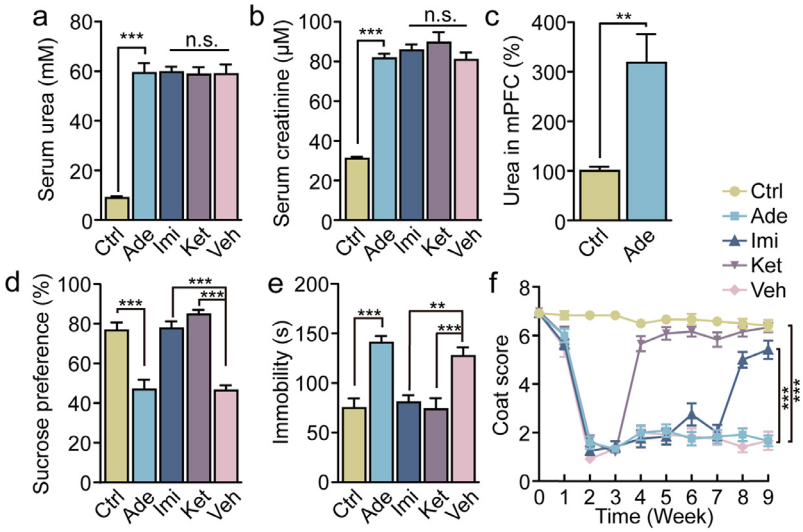

Fig. 2. High urea causes depression in CKD mice. a–f Adenine-induced mouse model ($n = 12$). a, Serum urea level of mice. b, Serum creatinine level of mice. c, Urea level in mPFC. d, Sucrose preference test. e, Force swimming test. f, Coat score. One-way ANOVA test (a–f). Ctrl, control group. Ade, adenine-induced CKD mice group. Imi, imipramine administration. Ket, ketamine administration. Veh, vehicle (saline) administration.

stress from physical suffering due to CKD. Urea undergoes complicated intrarenal recycling that is mediated by urea transporters [28] (Supplementary Fig. 9a). By knocking out urea transporters, we can increase or decrease urea reabsorption by the kidney to manipulate the serum urea level [28]. Urea transporter As (A) are expressed predominantly in the descending limb of Henle's loops and the end of collecting ducts to reabsorb urea [29] (Supplementary Fig. 9a, d). Urea transporter B (B) is expressed in descending vasa recta to transport urea from the interstitial tissue to blood (Supplementary Fig. 9b, d) [18]. $A^{+/+};B^{-/-}$ mice show an approximately 2-fold higher serum urea level and mPFC urea levels than $A^{+/+};B^{+/+}$ mice (Fig. 3a, b and Supplementary Fig. 9b). We detected normal kidney function by serum creatinine (Fig. 3c). Serum uric acid level and electrolytes and kidney index were all intact as well (Supplementary Fig. 10a–g).

Similar to clues in our previous study [5], compared to their $A^{+/+};B^{+/+}$ littermates, $A^{+/+};B^{-/-}$ mice exhibited several abnormal behaviours, including despair longer immobility and shorter latency to immobility in forced swimming test and tail suspension tests (Fig. 3d and Supplementary Fig. 10m–o), anhedonia (less preference to sucrose, Fig. 3e), low motivation (longer latency to food in novelty suppressed feeding test with normal appetite, Fig. 3f and Supplementary Fig. 10l) without motor defects (no shortness of total distance in open field test, Supplementary Fig. 10h). They also showed anxiety-like behaviours (less time in the central zone in open field test and less time in elevated plus-maze. Supplementary Fig. 10i and Fig. 3g), corresponding to anxiety symptoms in CKD patients (Fig. 1b). We also observed a bad fur condition and less grooming behaviour (coat score assay and splash test, Fig. 3h, i). The above behavioural tests have demonstrated the presence of depression-like behaviour in $A^{+/+};B^{-/-}$ mice.

Further urea transporter A deletion abolished the effect of urea transporter B deletion on the blood and mPFC urea levels (Fig. 3a, b, Supplementary Fig. 9c). $A^{-/-};B^{-/-}$ mice showed completely normal behaviour as do $A^{+/+};B^{+/+}$ mice, in all tests that we measured (Fig. 3c–f, Supplementary Fig. 10h–o). Therefore, the depression-like behaviour of $A^{+/+};B^{-/-}$ mice could be completely rescued by reducing urea back to normal levels.

Impairment of synaptic plasticity in mPFC is considered to be the core of depression [30], so we tested the effect of urea on LTP in acute brain slices. Adding urea lowered field excitatory postsynaptic potentials (fEPSPs) peak amplitude back to the baseline in ~20 min, suggesting that urea directly impairs LTP maintenance in the mPFC (Fig. 3j). However, urea did not change either frequency or amplitude of spontaneous miniature excitatory postsynaptic currents (mEPSCs) in layer V pyramidal neurons (Supplementary Fig. 12), which suggests that urea does not affect basal synaptic transmission at synapses. Together, high urea causes depression-like behaviour and impairs synaptic plasticity in the mPFC.

The impairment of LTP maintenance is mainly due to dysfunction of protein synthesis to form new neuronal structures [31–33]. Moreover, PFC from patients or rodents with depression displaced loss of neuronal spines, dendrites and synapses [34–36]. We measured structural proteins in mPFC of CKD mice, including MAP2, a marker of dendrites, Synapsin-1, a marker of pre-synapses, and PSD95, a marker of post-synapses. Synapsin-1 and PSD95 were both down-regulated in the CKD group, which suggested loss of synapses (Supplementary Fig. 7o, p). Antidepressants increased the expression of all tested proteins (Supplementary Fig. 7o, p). PSD95, Synapsin-1 and MAP2 were also decreased in $A^{+/+};B^{-/-}$ mice compared to the other two genotypes (Fig. 3k and Supplementary Fig. 10r, 11). In primary cultures of mPFC neurons, urea administration dose-dependently decreased PSD95, Synapsin-1 and MAP2 expression (Fig. 3l and Supplementary Fig. 10s). These data show that urea caused loss of synapses and dendrites in the formation of LTP.

3.4. Inhibition of mTORC1-S6K pathway is necessary in LTP impairment and depression induced by urea

The mammalian target of rapamycin (mTOR) kinase, as part of mTOR complex 1 (mTORC1), serves a key role in protein metabolism: it senses amino acid levels and controls protein synthesis [37]. Several clues have pointed to the mTORC1-S6K pathway. First, LTP maintenance needs dendritic protein synthesis that is regulated by the mTORC1-S6K pathway [38–40]. Second, suppression of the mTORC1-S6K pathway in the mPFC is involved in the molecular mechanism of depression [25,41–43]. Third, mTORC1 is the sensor of several amino acids levels [37], so it might be the sensor of their end-product urea as well.

Thus, we tested and found decreases in the phosphorylation of the mTOR target p70 S6K and its substrate p70 S6 in mPFC of CKD mice, but the phosphorylation level of mTOR was not decreased

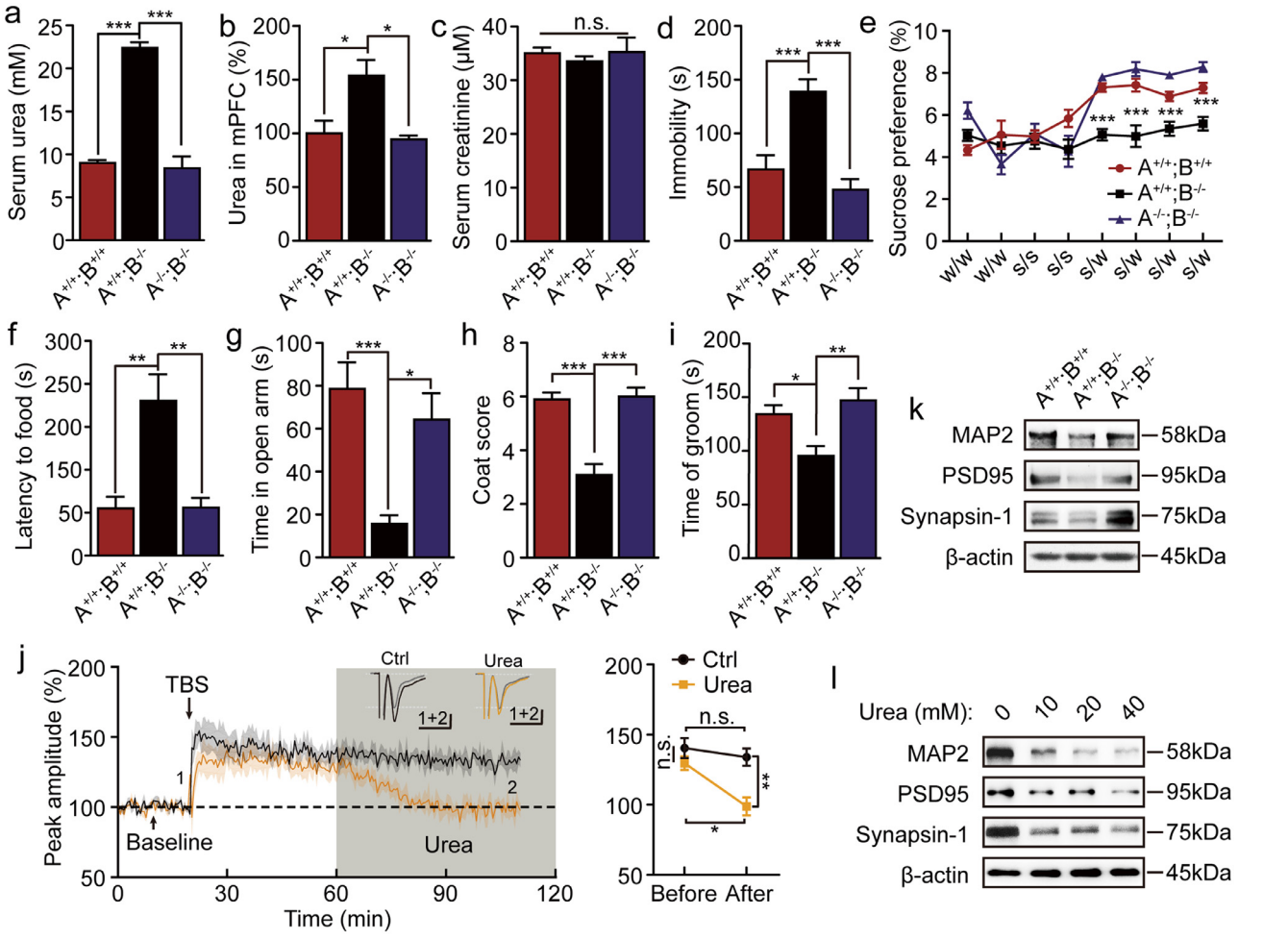

Fig. 3. Uremic toxin urea induces depression-like behaviour, LTP impairment and synapses loss. a–i, j, $A^{+/+};B^{+/+}$ mice *vs* $A^{+/+};B^{-/-}$ mice *vs* $A^{-/-};B^{-/-}$ mice. a, Serum urea level ($n = 4$). b, Urea level in mPFC ($n = 4$). c, Serum creatinine level ($n = 4$). d, Immobility in force swimming test ($n = 12,12,11$). e, 8-day sucrose preference test, w/w, water/water; s/s, sucrose/sucrose; s/w, sucrose/water ($n = 11,12,11$). f, Latency to food in novelty-suppressing feeding test ($n = 6,6,7$). g, Time in open arms in elevated plus maze ($n = 8,8,6$). h, Coat score ($n = 9,12,8$). i, Total grooming time in splash test ($n = 10,11,10$). j, Urea (20 mM) suppressed LTP in mPFC. Left, representative traces and LTP time course. Calibration bars are 50 pA, 50 ms; right, summary graphs of LTP magnitude. **k**, Expression of PSD95, Synapsin-1 and MAP2 *in vivo* by Western blot. l, Dose-dependent effect of urea on expression of PSD95, Synapsin-1, and MAP2 *in vitro* by Western blot. One-way ANOVA test (a–i), two-way ANOVA test (**j**).

(Fig. 4a, Supplementary Fig. 7p). Therefore, CKD mice had suppression of the mTORC1-S6K pathway in the mPFC. We also detected a decreased phosphorylation level of S6K and S6 in $A^{+/+};B^{-/-}$ mice compared to the other two genotypes. (Fig. 4b, Supplementary Fig. 10r). It confirmed that the direct effect of urea on neurons *in vitro*. Urea dose-dependently suppressed the mTORC1-S6K pathway in primary cultures of mouse mPFC neurons (Fig. 4c, Supplementary Fig. 10s). The effect of urea was independent of high osmotic stimulation, as assessed by using mannitol as a control (Supplementary Fig. 10p). In the time domain, the phosphorylation level of S6K and S6 were decreased from 0.5 h, and *p*-S6K reached its trough at 1 h ahead of *p*-S6, which reached its trough at 2 h (Supplementary Fig. 10q).

We then tested whether the mTORC1-S6K pathway is essential for urea to cause LTP impairment and depression-like behaviour. We created an adeno-associated virus carrying constitutively active S6K (AAV2-S6K^{ac}) (Fig. 4d and Supplementary Fig. 6b), and injected it into the mPFC to rescue the urea-induced decreased phosphorylation of S6 (Fig. 4d, e and Supplementary Fig. 14p). MAP2, Synapsin-1 and PSD95 were increased as down-stream proteins of S6 (Fig. 4e and Supplementary Fig. 13t, v, Fig. 14p). In healthy mice, the AAV2-S6K^{ac} had neither an effect on kidney nor a change of LTP (Supplementary Fig. 12a–i, u). In behavioural tests, the AAV2-S6K^{ac} only increased the appetite to food and times of rearing in healthy mice without changing other depression-related behaviours (Supplementary Fig. 13j–s). But in $A^{+/+};B^{-/-}$ mice, the AAV2-S6K^{ac} prevented LTP from impairment by urea (Fig. 4f), and it rescued core symptoms of depression with intact motor ability (Fig. 4g–k and Supplementary Fig. 14j–o). Not surprisingly, AAV-S6K^{ac} injected into mPFC did not affect urea level or other kidney markers in mice (Supplementary Fig. 13a–i and Supplementary Fig. 14a–g).

Ketamine could elevate the activity of mTORC1-S6K pathway in mPFC to reverse depression [25]. To further confirm the necessity of the mTORC1-S6K pathway, we treated $A^{+/+}$; $B^{-/-}$ mice with ketamine shots (Supplementary Fig. 6c). Compared with vehicle administration, ketamine-treated mice showed improved preference to sucrose solution (Fig. 4l). They showed less immobility in forced swimming and tail suspension tests without a defect of motor ability (Fig. 4m, Supplementary Fig. 15b–e, h–j). Ketamine also rescued anxiety-like behaviour (Fig. 4n) and motivation to food (Fig. 4o, Supplementary Fig. 15g). They also exhibited longer grooming behaviour and better fur appearance (Fig. 4p, Supplementary Fig. 15f).

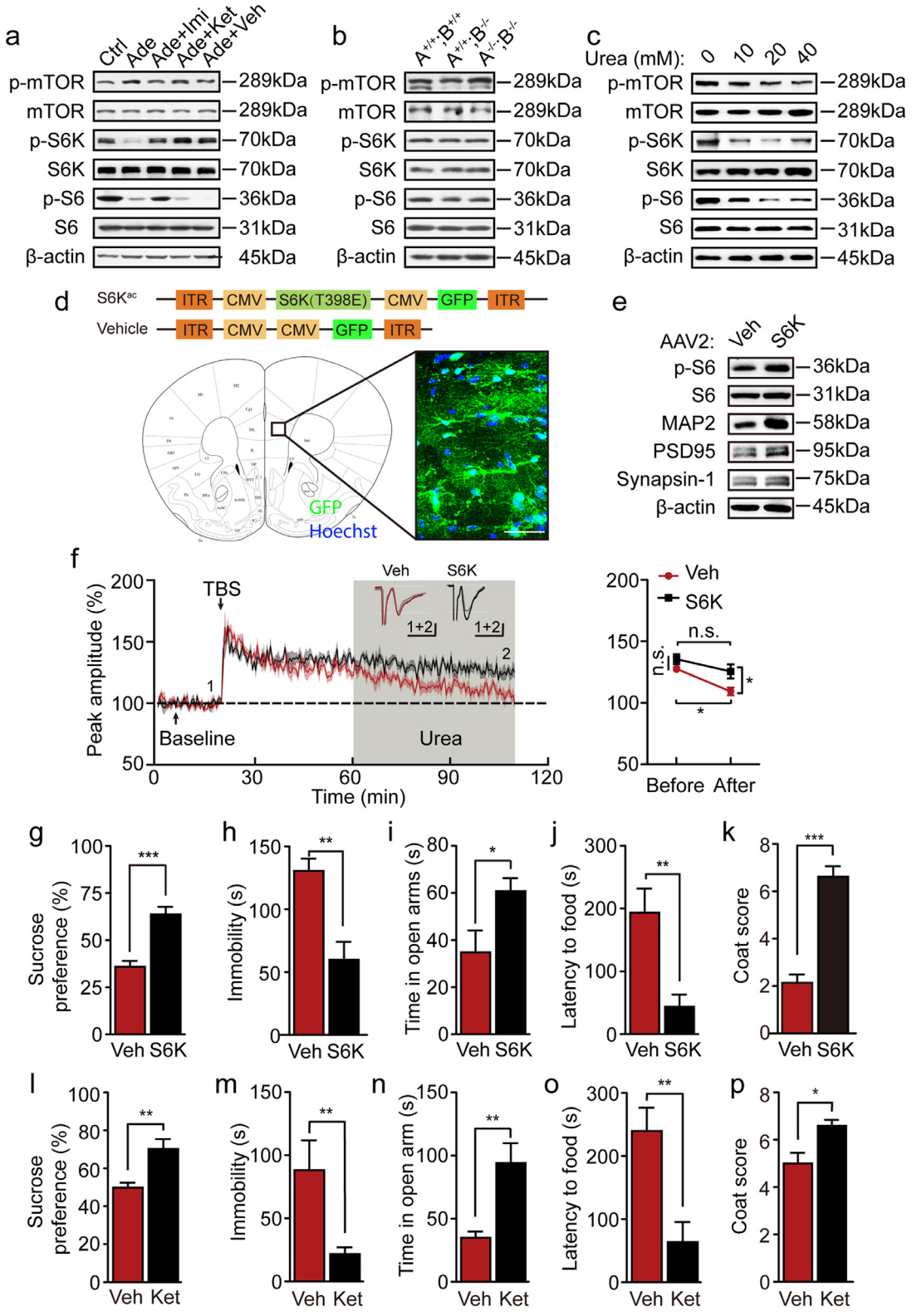

Fig. 4. mTORC1-S6K pathway is implicated in the effect of urea. a, mTORC1-S6K pathway in mPFC of adenine-induced CKD mice by Western blot. b, mTORC1-S6K pathway in mPFC of $A^{+/+};B^{+/+}$ mice, $A^{+/+};B^{-/-}$ mice and $A^{-/-};B^{-/-}$ mice by Western blot . c, Dose-dependent effect of urea on mTORC1-S6K pathway *in vitro* by Western blot. d, Schematic of the AAV vector encoding constitutive active S6K ($S6K^{ac}$), vehicle, and the injection site into the mPFC (white bar, 20 μm). e, Phosphorylation level of S6 and expression of PSD95, Synapsin-1 and MAP2 on mPFC of $A^{+/+};B^{-/-}$ mice injected of $S6K^{ac}$ or vehicle by Western blot. f, Urea (20 mM) could not suppress LTP on slices expressing $S6K^{ac}$. Left, representative traces and LTP time course. Calibration bars are 50 pA, 50 ms; right, summary graphs of LTP magnitude. g–k, Behaviour tests of $A^{+/+};B^{-/-}$ mice injected of $S6K^{ac}$ or vehicle virus in mPFC. g, Sucrose preference test ($n=6$). h, Time in open arms in elevated plus maze ($n=6$). i, Immobility in force swimming test ($n=4,5$). j, Latency to food in novelty-suppressing feeding test ($n=6$). k, Coat score ($n=8$). l–p, Behaviour tests of $A^{+/+};B^{-/-}$ mice administrated with ketamine or vehicle. l, Sucrose preference test. m, Time in open arms in elevated plus-maze. n, Immobility in force swimming test. o, Latency to food in novelty-suppressing feeding test. p, Coat score. (l–p, $n=5$.) Student's *t*-test (g–p), two-way ANOVA test (f).

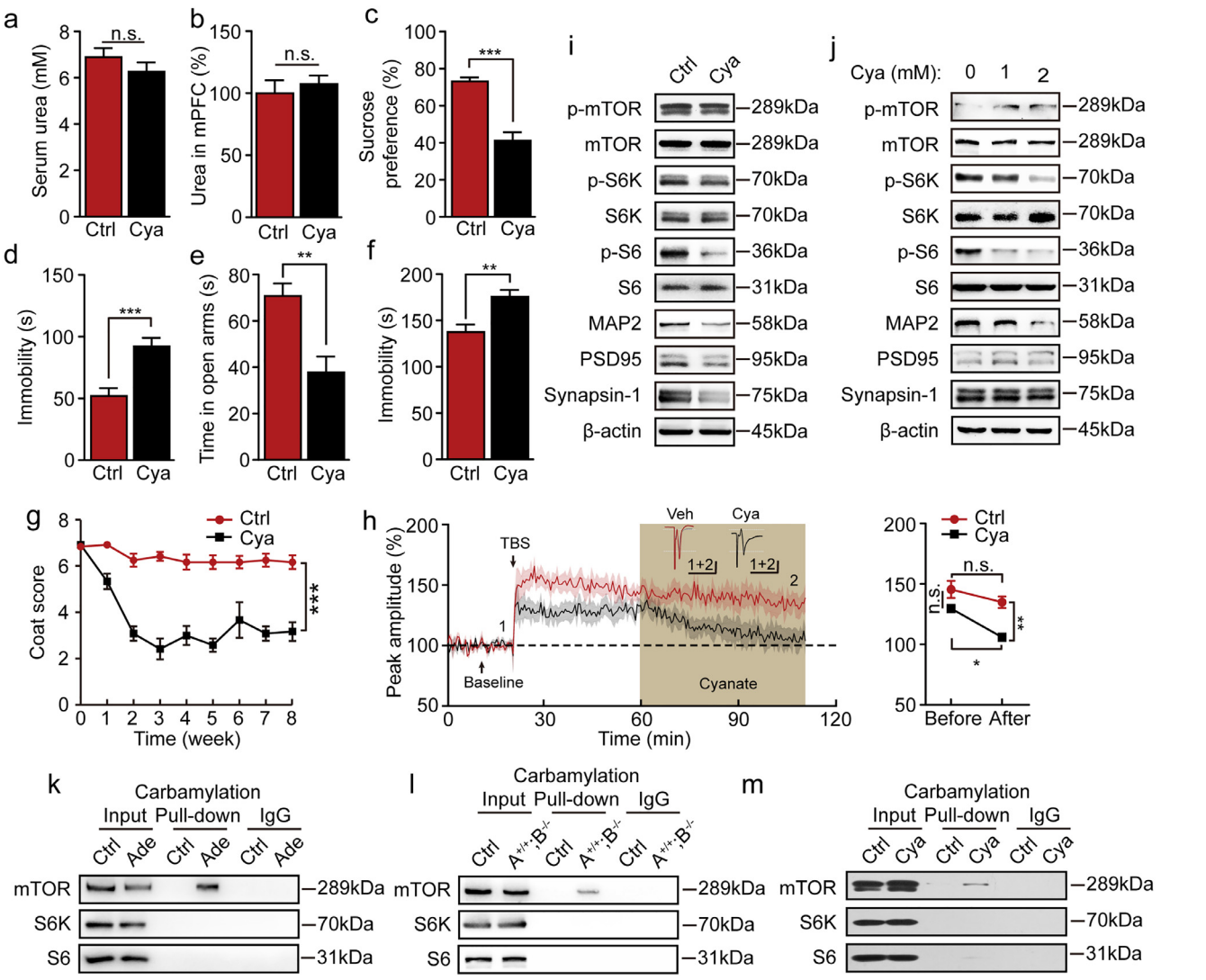

Fig. 5. Mechanism and target of urea. a-g, Effect of cyanate on mice. a, Serum urea level in cyanate-feeding mice ($n = 11,12$). b, mPFC urea level in cyanate-feeding mice. c, Sucrose preference test. d, Immobility in force swimming test. e, Time in open arms in elevated plus-maze. f, Immobility in tail suspension test. g, Coat score. (b–g, $n = 12$.) h, Cyanate (2 mM) suppressed LTP in mPFC. Left, representative traces and LTP time course. Calibration bars are 50 pA, 50 ms; right, summary graphs of LTP magnitude. i, Changes of mTORC1-S6K pathway and markers of synapses in mPFC of cyanate-feeding mice by Western blot. j, Dose-dependent effect of cyanate on mTORC1-S6K pathway and markers of synapses *in vitro* by Western blot. k–m, Target of urea/cyanate, carbamylation pull-down on proteins distracted from mPFC. k, Adenine-induced CKD mice. l, $A^{+/+};B^{+/+}$ mice, $A^{+/+};B^{-/-}$ mice. m, Cyanate-feeding mice. Student's *t*-test (a–g), two-way ANOVA test (h).

3.5. Mechanism and target of urea on mTORC1-S6K pathway suppression

The next question is how the accumulation of urea suppresses the mTORC1/S6K pathway. Though urea is the end product that is not catalysed by mammalian cells, it leads to the non-enzymatic hydrolysate cyanate (Supplementary Fig. 16a). To determine whether urea interferes in the mTORC1-S6K signalling pathway by its byproduct cyanate, we administrated cyanate to mice through drinking water and tested their behaviours (Supplementary Fig. 6d). Cyanate drinking did not change renal function or urea level, either in serum or in mPFC (Fig. 5a, b, Supplementary Fig. 16b–i), and it did not affect kidney histology (Supplementary Fig. 16). After exposure to cyanate, in behavioural aspects, mice exhibited anhedonia, despair and anxiety but no change in motor activity (Fig. 5c–f, Supplementary Fig. 16j–p). The coat score, reflecting less grooming behaviour, was measured every week as a monitor of depression (Fig. 5g). Cyanate also damaged LTP maintenance in mPFC (Fig. 5h). Same as with urea administration, mEPSCs were totally intact after cyanate stimulation in the mPFC (Supplementary Fig. 18). The mTORC1-S6K pathway was suppressed, and structure-related proteins were down-regulated (Fig. 5i, Supplementary Fig. 16r). Accordingly, cyanate dose-dependently suppressed the mTORC1-S6K pathway *in vitro* (Fig. 5j, Supplementary Fig. 16s), and the effect of extra osmotic pressure and sodium ion was excluded (Supplementary Fig. 16q). Together, the impact of cyanate equals that of urea, so urea could work through its hydrolysate cyanate.

The target protein of urea and cyanate is the last vital question. Cyanate modulates certain types of amino acid residues, which is called carbamylation, a type of post-translational modification [44]. Carbamylation of some life-vital proteins could lead to dysfunction of processes that involve these proteins [44–47]. Besides, there is an interesting paradox in our above data. p70 S6K is a downstream effector of mTORC1 and a direct substrate of mTOR kinase [48–51] and phosphorylation of p70 S6K at the Thr389 residue is catalysed by mTOR. In our data, *p*-S6K was decreased, whereas, total expression of mTOR was unchanged and the phosphorylated

mTOR, representing the active mTOR, was not decreased at all but even elevated sometime (Figs. 4a–c, 5i, j, Supplementary Figs. 7p 10p–s, 16q–s). Based on the above two reasons, we therefore pulled down all carbamylated proteins and checked whether mTOR was modified. In the mPFC of CKD mice, $A^{+/+};B^{-/-}$ mice and cyanate-exposed mice, all mTOR was carbamylated (Fig. 5k–m). In contrast, as down-stream proteins, neither S6K nor S6 were carbamylated in any experiments. These data suggest that urea and cyanate could modulate mTOR protein and decrease its kinase activity. In other words, carbamylation of mTOR could be the way in which a cell senses the concentration of urea.

4. Discussion

In the current study, we discovered and proved that urea accumulation could induce depression directly, bypassing psychosocial stress. We also found the underlying mechanism, which demonstrated that urea or cyanate carbamylates mTOR to inhibit the mTORC1-S6K dependent dendritic protein synthesis, inducing impairment of synaptic plasticity in mPFC and depression-like behaviour.

We proved the toxicity of urea to the nervous system by sufficient experiments for the first time. Previous studies have focused more on the fact that urea exacerbates the progression of the disease or plays a role in certain complications. It has also been reported that high urea and its hydrolysate cyanate have toxicity in other cells and tissues. Urea induces the expression of pro-apoptotic proteins in human aortic endothelial cells [52,53], resulting in increased mitochondrial ROS production and activation of pro-inflammatory pathways which deteriorates the quality of life of patients with chronic kidney disease [54–56]. A dose-dependent relationship with impaired insulin signalling has been observed when a high urea concentration of 10∼40 mM is added in cultured adipocytes [4]. Carbamylation of LDL decreases its recognition by the LDL receptor but increases uptake by macrophage scavenger receptor, thus driving atherosclerosis [47]. Carbamylated albumin drives interstitial fibrosis [57]. Diffusion of urea into the gut lumen drives breakdown of epithelial tight junctions [58] and alters the gut microbiome and favours expansion of bacterial families that produce uremic toxins in CKD [59]. Our study enriches the evidence and provides a complete signal pathway for urea toxicity. We further proved that it is directly related to depression in the absence of any stress. Therefore, we suggest that urea should be considered as an independent factor causing disease directly.

Research has significantly advanced our understanding of urea toxicity at the cellular and systemic levels. Accumulating evidence suggests that elevated urea has a negative impact on CKD patient outcomes. Urea per se probably participates in the pathogenesis of cardiovascular disease, CKD progression, insulin resistance, intestinal disease, anaemia, and contributes to an overall accelerated ageing phenotype [60]. However, direct proof of the impact of elevated urea is currently lacking and will be difficult to ascertain, given the retention of other uremic toxins in CKD [61]. In this paper, the urea transporter B null mice and all urea transporters null mice provide us with proper tools to eliminate other interference factors. We have subtly controlled the concentration of urea through the knockout of the urea transporters. CKD is characterized by the progressive retention of metabolites normally excreted by the kidney, collectively termed “uremic toxins” including β2-microglobulin, indoxyl sulfate, homocysteine, uric acid, carboxymethyllysine, cystatin C, and parathyroid hormone, many of which have adverse effects on numerous organs [62] . Whereas almost all considered solutes affect one or more functions that contribute to the uremic syndrome and its complications, especially the susceptibility to cardiovascular damage, inflammation and fibrosis appeared to be targeted [63]. For the mental illness focused on this research, unlike CKD mice, short-term of UT-B knockout mice proven to have complete kidney function with a high urea level and without any other uremic toxins in our supplementary materials, especially without toxins that have been proven to be associated with neurological diseases. $A^{-/-};B^{-/-}$ mice, as a control, could exclude other potential confounding effects, such as the effects of extrarenal B deletion, discomfort of polyuria, etc. These two kinds of knockout mice are excellent tools for studying the independent toxicity of high urea better than other animal models.

Previously, the studies of carbamylation were mostly about structural and blood proteins [64]. Research has demonstrated that the neurotoxicity caused by cyanate is triggered by disruption of glutathione metabolism in neural tissue [65,66]. In this study, however, we discovered the potential role of cyanate and carbamylation on a signalling cascade. In this way, the effects of carbamylation can be very general and wide across different organs and tissues. Our results indicate that urea delivers organ-crosstalk information specifically from kidney to brain. A series of studies have noticed the kidney-brain communication, and found cytokines, chemokines etc. are the talking medium [67,68]. However, these substances are so general that they can be “talked” by lots of organs and tissues aside from the kidney. The urea level is very stable in almost all conditions, except in kidney dysfunction, which makes urea a reliable crosstalk language that only the kidney speaks.

However, some challenges remain in our study. First, to our knowledge, there is no method to control hydrolysis reaction *in vivo*, so we are not able to test the effect of urea without the existence of cyanate. Second, further data are needed to confirm the molecular mechanism on how mTOR senses urea. Third, LTP is a complex process that includes both presynaptic and postsynaptic mechanisms. Therefore, further study should focus on more precise effects of urea on synaptic plasticity. The fourth, further study should also focus on whether other brain regions that maybe impaired by urea, such as the limbic system, the reward system, etc. We speculate that the effects of urea accumulation on the nervous system may not only induce depression but also affect at least memory formation or recall.

As the clinical significance of this study, treatments need to be considered with the risks and benefits to patients in mind, including prescribing high urea dialysis and urea cream etc. to high serum urea level patients. The conventional view that urea is non-hazardous is based on a clinical trial at Mayo Clinic in the 1970s – they additionally elevated the urea level in CKD patients who had already had a high blood urea level and patients completely tolerated 50 mM urea [69]. Clinicians ignore the relationship between urea and other CKD complications. Patients who have a high urea level always have kidney dysfunction, which changes the pharmacokinetics of several antidepressants [70], and a reduced clearance of these antidepressants may easily cause an overdose. Moreover, some antidepressants, such as lithium, have remarkable kidney toxicity so that the therapy itself could further damage the kidney of CKD patients [71]. Therefore, it could be beneficial if single strict management of urea in CKD patients could be a potential therapy or prevention for depression.

Funding sources

This work was supported by NIH R01HD072074, National Natural Science Foundation of China grants 81770738, 81620108029 and 81330074, International Science & Technology Cooperation Program of China grant 2012DFA11070, the 111 Project, the Scientific and Technological Research Program of Chongqing Yuzhongqu Scientific and Technological Commission (20120202), Research Program of Chongqing National Health and Family Planning Commission (2012-1-038), and the Chongqing Science and Technology Commission (Project No. cstc2015jcyjA10036). Funding bodies had

no role in the design of the study and collection, analysis, and interpretation of data and in writing the manuscript and eventually in the decision to submit the manuscript.

Declaration of Competing Interest

The authors declare no competing interests.

CRediT authorship contribution statement

Hongkai Wang: Conceptualization, Data curation, Formal analysis, Writing - original draft. **Boyue Huang:** Formal analysis, Writing - review & editing. **Weiling Wang:** Data curation. **Trevor Flynn:** Data curation, Formal analysis. **Keqiong Li:** Data curation. **Li Yan:** Data curation. **Jianhua Ran:** Conceptualization, Funding acquisition, Supervision, Writing - review & editing. **Baoxue Yang:** Conceptualization, Funding acquisition, Supervision, Writing - review & editing.

Acknowledgement

The authors would like to thank Dr. Daqi Yu from School of Physics, Tianyu Zhang from School of Life Sciences, Bing Cao from School of Public Health, Peking University, Jingwei Song from Department of Statistics, University of California Los Angeles for enlightening conversation; Jingjie Li from Xi'an Jiaotong University, Junkui Shang from Capital Medical University, Chenyu Zhang and senior technician Mrs. Wenyuan Guo from School of Basic Medical Sciences, Peking University, Beian Dong and Yujiao Dou from Ion Channel Explorer Bioscience INC., Dr. Xingyu Zhang and Dr. Qiang Liu from the First People's Hospital of Chongqing Liang Jiang New Area for technologic assistance.

Supplementary materials

Supplementary material associated with this article can be found, in the online version, at doi:10.1016/j.ebiom.2019.09.049.

References

[1] He L, Fu M, Chen X, Liu H, Chen X, Peng X, et al. Effect of dialysis dose and membrane flux on hemoglobin cycling in hemodialysis patients. Hemodial Int 2015;19(2):263–9.
[2] Ivanovski O, Szumilak D, Nguyen-Khoa T, Ruellan N, Phan O, Lacour B, et al. The antioxidant N-acetylcysteine prevents accelerated atherosclerosis in uremic apolipoprotein E knockout mice. Kidney Int 2005;67(6):2288–94.
[3] Zhang Z, Dmitrieva NI, Park JH, Levine RL, Burg MB. High urea and NACL carbonylate proteins in renal cells in culture and *in vivo*, and high urea causes 8-oxoguanine lesions in their DNA. Proc Natl Acad Sci USA 2004;101(25):9491–6.
[4] D'Apolito M, Du X, Zong H, Catucci A, Maiuri L, Trivisano T, et al. Urea-induced ROS generation causes insulin resistance in mice with chronic renal failure. J Clin Invest 2010;120(1):203–13.
[5] Li X, Ran J, Zhou H, Lei T, Zhou L, Han J, et al. Mice lacking urea transporter UT-B display depression-like behavior. J Mol Neurosci 2011;46(2):362–72.
[6] Jiang T, Li Y, Layton AT, Wang W, Sun Y, Li M, et al. Generation and phenotypic analysis of mice lacking all urea transporters. Kidney Int 2017;91(2):338–51.
[7] Whiteford HA, Degenhardt L, Rehm J, Baxter AJ, Ferrari AJ, Erskine HE, et al. Global burden of disease attributable to mental and substance use disorders: findings from the global burden of disease study 2010. Lancet 2013;382(9904):1575–86.
[8] Caspi A, Sugden K, Moffitt TE, Taylor A, Craig IW, Harrington H, et al. Influence of life stress on depression: moderation by a polymorphism in the 5-HTT gene. Science 2003;301(5631):386–9.
[9] Pittenger C, Duman RS. Stress, depression, and neuroplasticity: a convergence of mechanisms. Neuropsychopharmacology 2008;33(1):88–109.
[10] Wells KB, Golding JM, Burnam MA. Psychiatric disorder in a sample of the general population with and without chronic medical conditions. Am J Psychiatry 1988;145(8):976–81.
[11] Aneshensel CS, Frerichs RR, Huba GJ. Depression and physical illness: a multiwave, nonrecursive causal model. J Health Soc Behav 1984:350–71.
[12] Krishnan KRR, Delong M, Kraemer H, Carney R, Spiegel D, Gordon C, et al. Comorbidity of depression with other medical diseases in the elderly. Biol Psychiatry 2002;52(6):559–88.
[13] Steptoe A. Depression and physical illness. Cambridge University Press; 2006.
[14] Robinson RG, Jorge RE. Post-Stroke depression: a review. Am J Psychiatry 2015:appiajp201515030363.
[15] McDonald WM, Richard IH, DeLong MR. Prevalence, etiology, and treatment of depression in Parkinson's disease. Biol Psychiatry 2003;54(3):363–75.
[16] Jia T, Olauson H, Lindberg K, Amin R, Edvardsson K, Lindholm B, et al. A novel model of adenine-induced tubulointerstitial nephropathy in mice. BMC Nephrol 2013;14(1):116.
[17] El-Gamal D, Holzer M, Gauster M, Schicho R, Binder V, Konya V, et al. Cyanate is a novel inducer of endothelial icam-1 expression. Antioxid Redox Signal 2012;16(2):129–37.
[18] Yang B, Bankir L, Gillespie A, Epstein CJ, Verkman AS. Urea-selective concentrating defect in transgenic mice lacking urea transporter UT-B. J Biol Chem 2002;277(12):10633–7.
[19] Jiang T, Li Y, Layton AT, Wang W, Sun Y, Li M, et al. Generation and phenotypic analysis of mice lacking all urea transporters. Kidney Int 2016.
[20] Schalm SS, Blenis J. Identification of a conserved motif required for mTOR signaling. Curr Biol 2002;12(8):632–9.
[21] Trinh-Trang-Tan MM, Lasbennes F, Gane P, Roudier N, Ripoche P, Cartron JP, et al. UT-B1 proteins in rat: tissue distribution and regulation by antidiuretic hormone in kidney. Am J Physiol Renal Physiol 2002;283(5):F912–22.
[22] Drevets WC, Price JL, Simpson JR, Todd RD, Reich T, Vannier M, et al. Subgenual prefrontal cortex abnormalities in mood disorders. Nature 1997;386(6627):824–7.
[23] Rajkowska G, Miguel-Hidalgo JJ, Wei J, Dilley G, Pittman SD, Meltzer HY, et al. Morphometric evidence for neuronal and glial prefrontal cell pathology in major depression. Biol Psychiatry 1999;45(9):1085–98.
[24] Monleon S, D'Aquila P, Parra A, Simon VM, Brain PF, Willner P. Attenuation of sucrose consumption in mice by chronic mild stress and its restoration by imipramine. Psychopharmacology 1995;117(4):453–7.
[25] Li N, Lee B, Liu RJ, Banasr M, Dwyer JM, Iwata M, et al. mTOR-dependent synapse formation underlies the rapid antidepressant effects of NMDA antagonists. Science 2010;329(5994):959–64.
[26] Autry AE, Adachi M, Nosyreva E, Na ES, Los MF, Cheng PF, et al. NMDA receptor blockade at rest triggers rapid behavioural antidepressant responses. Nature 2011;475(7354):91–5.
[27] Surget A, Saxe M, Leman S, Ibarguen-Vargas Y, Chalon S, Griebel G, et al. Drug-dependent requirement of hippocampal neurogenesis in a model of depression and of antidepressant reversal. Biol Psychiatry 2008;64(4):293–301.
[28] Bankir L, Yang B. New insights into urea and glucose handling by the kidney, and the urine concentrating mechanism. Kidney Int 2012;81(12):1179–1198.
[29] Fenton RA, Chou C-L, Stewart GS, Smith CP, Knepper MA. Urinary concentrating defect in mice with selective deletion of phloretin-sensitive urea transporters in the renal collecting duct. Proc Natl Acad Sci USA 2004;101(19):7469–74.
[30] Duman RS, Aghajanian GK, Sanacora G, Krystal JH. Synaptic plasticity and depression: new insights from stress and rapid-acting antidepressants. Nat Med 2016;22(3):238–49.
[31] Engert F, Bonhoeffer T. Dendritic spine changes associated with hippocampal long-term synaptic plasticity. Nature 1999;399(6731):66–70.
[32] Geinisman Y, Detoledo-Morrell L, Morrell F, Persina IS, Beatty MA. Synapse restructuring associated with the maintenance phase of hippocampal long-term potentiation. J Comp Neurol 1996;368(3):413–23.
[33] Toni N, Buchs PA, Nikonenko I, Bron CR, Muller D. LTP promotes formation of multiple spine synapses between a single axon terminal and a dendrite. Nature 1999;402(6760):421–5.
[34] Kang HJ, Voleti B, Hajszan T, Rajkowska G, Stockmeier CA, Licznerski P, et al. Decreased expression of synapse-related genes and loss of synapses in major depressive disorder. Nat Med 2012;18(9):1413–17.
[35] Radley JJ, Rocher AB, Miller M, Janssen WG, Liston C, Hof PR, et al. Repeated stress induces dendritic spine loss in the rat medial prefrontal cortex. Cereb Cortex 2006;16(3):313–20.
[36] Liu RJ, Aghajanian GK. Stress blunts serotonin- and hypocretin-evoked EPSCs in prefrontal cortex: role of corticosterone-mediated apical dendritic atrophy. Proc Natl Acad Sci USA 2008;105(1):359–64.
[37] Efeyan A, Comb WC, Sabatini DM. Nutrient-sensing mechanisms and pathways. Nature 2015;517(7534):302–10.
[38] Cammalleri M, Lutjens R, Berton F, King AR, Simpson C, Francesconi W, et al. Time-restricted role for dendritic activation of the mTOR-p70S6K pathway in the induction of late-phase long-term potentiation in the CA1. Proc Natl Acad Sci USA 2003;100(24):14368–73.
[39] Tang SJ, Reis G, Kang H, Gingras AC, Sonenberg N, Schuman EM. A rapamycin-sensitive signaling pathway contributes to long-term synaptic plasticity in the hippocampus. Proc Natl Acad Sci USA 2002;99(1):467–72.
[40] Gong R, Park CS, Abbassi NR, Tang SJ. Roles of glutamate receptors and the mammalian target of rapamycin (mTOR) signaling pathway in activity-dependent dendritic protein synthesis in hippocampal neurons. J Biol Chem 2006;281(27):18802–15.
[41] Jernigan CS, Goswami DB, Austin MC, Iyo AH, Chandran A, Stockmeier CA, et al. The mTOR signaling pathway in the prefrontal cortex is compromised in major depressive disorder. Prog Neuropsychopharmacol Biol Psychiatry 2011;35(7):1774–9.
[42] Ota KT, Liu RJ, Voleti B, Maldonado-Aviles JG, Duric V, Iwata M, et al. REDD1 is essential for stress-induced synaptic loss and depressive behavior. Nat Med 2014;20(5):531–5.

[43] Dwyer JM, Maldonado-Aviles JG, Lepack AE, DiLeone RJ, Duman RS. Ribosomal protein S6 kinase 1 signaling in prefrontal cortex controls depressive behavior. Proc Natl Acad Sci USA 2015;112(19):6188–93.
[44] Berg AH, Drechsler C, Wenger J, Buccafusca R, Hod T, Kalim S, et al. Carbamylation of serum albumin as a risk factor for mortality in patients with kidney failure. Sci Transl Med 2013;5(175):175ra29.
[45] Apostolov EO, Ray D, Savenka AV, Shah SV, Basnakian AG. Chronic uremia stimulates LDL carbamylation and atherosclerosis. J Am Soc Nephrol 2010;21(11):1852–7.
[46] Holzer M, Birner-Gruenberger R, Stojakovic T, El-Gamal D, Binder V, Wadsack C, et al. Uremia alters HDL composition and function. J Am Soc Nephrol 2011;22(9):1631–41.
[47] Wang Z, Nicholls SJ, Rodriguez ER, Kummu O, Horkko S, Barnard J, et al. Protein carbamylation links inflammation, smoking, uremia and atherogenesis. Nat Med 2007;13(10):1176–84.
[48] Chung J, Kuo CJ, Crabtree GR, Blenis J. Rapamycin-FKBP specifically blocks growth-dependent activation of and signaling by the 70 kd S6 protein kinases. Cell 1992;69(7):1227–36.
[49] Kuo CJ, Chung J, Fiorentino DF, Flanagan WM, Blenis J, Crabtree GR. Rapamycin selectively inhibits interleukin-2 activation of p70 S6 kinase. Nature 1992;358(6381):70–3.
[50] Price DJ, Grove JR, Calvo V, Avruch J, Bierer BE. Rapamycin-induced inhibition of the 70-kilodalton S6 protein kinase. Science 1992;257(5072):973–977.
[51] Calvo V, Crews CM, Vik TA, Bierer BE. Interleukin 2 stimulation of p70 S6 kinase activity is inhibited by the immunosuppressant rapamycin. Proc Natl Acad Sci USA 1992;89(16):7571–5.
[52] Vanholder R, Massy Z, Argiles A, Spasovski G, Verbeke F, Lameire N. Chronic kidney disease as cause of cardiovascular morbidity and mortality. Nephrol Dial Transplant 2005;20(6):1048–56.
[53] Caravaca F, Martin MV, Barroso S, Ruiz B, Hernandez-Gallego R. Do inflammatory markers add predictive information of death beyond that provided by age and comorbidity in chronic renal failure patients? Nephrol Dial Transplant 2006;21(6):1575–81.
[54] Yip J, Facchini FS, Reaven GM. Resistance to insulin-mediated glucose disposal as a predictor of cardiovascular disease. J Clin Endocrinol Metab 1998;83(8):2773–6.
[55] Bodlaj G, Berg J, Pichler R, Biesenbach G. Prevalence, severity and predictors of HOMA-estimated insulin resistance in diabetic and nondiabetic patients with end-stage renal disease. J Nephrol 2006;19(5):607–12.
[56] D'Apolito M, Du X, Pisanelli D, Pettoello-Mantovani M, Campanozzi A, Giacco F, et al. Urea-induced ROS cause endothelial dysfunction in chronic renal failure. Atherosclerosis 2015;239(2):393–400.
[57] Shaykh M, Pegoraro AA, Mo W, Arruda JA, Dunea G, Singh AK. Carbamylated proteins activate glomerular mesangial cells and stimulate collagen deposition. J Lab Clin Med 1999;133(3):302–8.
[58] Al-Sadi R, Boivin M, Ma T. Mechanism of cytokine modulation of epithelial tight junction barrier. Front Biosci (Landmark Ed) 2009;14:2765–78.
[59] Wang F, Jiang H, Shi K, Ren Y, Zhang P, Cheng S. Gut bacterial translocation is associated with microinflammation in end-stage renal disease patients. Nephrol (Carlton, Vic) 2012;17(8):733–8.
[60] White WE, Yaqoob MM, Harwood SM. Aging and uremia: is there cellular and molecular crossover? World J Nephrol 2015;4(1):19–30.
[61] Lau WL, Vaziri ND. Urea, a true uremic toxin: the empire strikes back. Clin Sci 2017;131(1):3–12.
[62] Stinghen AE, Massy ZA, Vlassara H, Striker GE, Boullier A. Uremic toxicity of advanced glycation end products in CKD. J. Am. Soc. Nephrol. 2016;27(2):354–70.
[63] Vanholder R, Pletinck A, Schepers E, Glorieux G. Biochemical and clinical impact of organic uremic retention solutes: a comprehensive update. Toxins (Basel) 2018;10(1).
[64] Delanghe S, Delanghe JR, Speeckaert R, Van Biesen W, Speeckaert MM. Mechanisms and consequences of carbamoylation. Nat Revi Nephrol 2017;13(9):580–93.
[65] Sokolowska M, Lorenc-Koci E, Bilska A, Iciek M. The effect of lipoic acid on cyanate toxicity in different structures of the rat brain. Neurotox Res 2013;24(3):345–57.
[66] Tor-Agbidye J, Palmer VS, Spencer PS, Craig AM, Blythe LL, Sabri MI. Sodium cyanate alters glutathione homeostasis in rodent brain: relationship to neurodegenerative diseases in protein-deficient malnourished populations in Africa. Brain Res 1999;820(1–2):12–19.
[67] Lu R, Kiernan MC, Murray A, Rosner MH, Ronco C. Kidney-brain crosstalk in the acute and chronic setting. Nat Rev Nephrol 2015;11(12):707–19.
[68] Bugnicourt JM, Godefroy O, Chillon JM, Choukroun G, Massy ZA. Cognitive disorders and dementia in CKD: the neglected kidney-brain axis. J Am Soc Nephrol 2013;24(3):353–63.
[69] Johnson WJ, Hagge WW, Wagoner RD, Dinapoli RP, Rosevear JW. Effects of urea loading in patients with far-advanced renal failure. Mayo Clin Proc 1972;47(1):21–9.
[70] Nagler EV, Webster AC, Vanholder R, Zoccali C. Antidepressants for depression in stage 3–5 chronic kidney disease: a systematic review of pharmacokinetics, efficacy and safety with recommendations by European renal best practice (ERBP). Nephrol Dial Transplant 2012;27(10):3736–45.
[71] Boton R, Gaviria M, Batlle DC. Prevalence, pathogenesis, and treatment of renal dysfunction associated with chronic lithium therapy. Am J Kidney Dis 1987;10(5):329–45.